An analytical approach to bistable biological circuit discrimination using real algebraic geometry

Dan Siegal-Gaskins[1], Elisa Franco[2], Tiffany Zhou[1], and Richard M. Murray[1,3]

1. Division of Biology and Biological Engineering, California Institute of Technology, Pasadena, CA, USA
2. Department of Mechanical Engineering, University of California at Riverside, Riverside, CA, USA
3. Department of Control and Dynamical Systems, California Institute of Technology, Pasadena, CA, USA

1 Summary

Small biomolecular circuits with two distinct and stable steady states have been identified as essential components in a wide range of biological networks, with a variety of mechanisms and topologies giving rise to their important bistable property. Understanding the differences between circuit implementations is an important question, particularly for the synthetic biologist faced with the challenge of determining which bistable circuit design out of many is best for their specific application. In this work we explore the applicability of Sturm's theorem—a tool from 19th-century real algebraic geometry—to comparing "functionally equivalent" bistable circuits without the need for numerical simulation. We consider two genetic toggle variants and two different positive feedback circuits, and show how specific topological properties present in each type of circuit can serve to increase the size of their operational range. The demonstrated predictive power and ease of use of Sturm's theorem suggests that algebraic geometric techniques may be underutilized in biomolecular circuit analysis.

2 Key words

synthetic biology; biological circuit; bistability; algebraic geometry; Sturm's theorem

3 Introduction

The field of synthetic biology has rapidly matured to the point where it is now possible to produce complex synthetic networks with prescribed functions and level of performance [1]. As in other fields of engineering, advances have been enabled by the use of small interchangeable modules that are "functionally equivalent" from an input-output perspective [2]. Bistable circuits—which play a role in essential biological processes including cell fate specification [3], cell cycle progression [4], and apoptosis [5]—make up a particularly large and diverse functionally equivalent set [6]. Effectively characterizing and comparing these biocircuits is crucial for determining which architecture is in some sense optimal for a particular context.

Ordinary differential equation (ODE) models can be powerful tools for contrasting different biocircuits' "dynamic phenotypes" (see, e.g., [7]); however, as circuit size increases, the usefulness of such models can be limited by their complexity. Many of the relevant parameters are often unknown, and while computational

techniques have advantages, analytical criteria that focus on topology can provide a more exact assessment of a module's properties [8, 9]. A novel analytical tool that can provide topology-based insights can be found in Sturm's theorem [10], developed in 1835 as a solution to the problem of finding the number of real roots of an algebraic equation with real coefficients over a given interval. Despite its predictive power, this "gem of 19th century algebra and one of the greatest discoveries in the theory of polynomials" [11] remains unexploited as a tool for synthetic biology.

In this work we demonstrate an approach to bistable circuit discrimination based on Sturm's theorem that gives boundaries of the regions of bistability as exact analytic expressions, eliminating the need for numerical simulation. We compare the regions of bistability for two variants of the classic double-negative toggle switch as well as two positive feedback circuits, one of which is based on the bacteriophage λ promoter P_{RM}. Overall our results demonstrate the usefulness of algebraic geometric techniques for studying functionally equivalent bistable circuits and suggest a new and simple-to-implement method for choosing between them for synthetic biological applications.

4   Mathematical preliminaries

4.1   Sturm's theorem

Sturm's theorem gives the number of distinct real roots of a univariate polynomial $f(x)$ in a particular interval. To apply the theorem, we must first construct the *Sturm sequence*, a set of polynomials $\mathcal{F} = \{f_0, f_1, \ldots, f_m\}$ defined as:

$$
\begin{aligned}
f_0 &= f(x), \\
f_1 &= f'(x), \\
f_2 &= -\mathrm{rem}(f_0, f_1), \\
f_3 &= -\mathrm{rem}(f_1, f_2), \\
&\vdots \\
f_m &= -\mathrm{rem}(f_{m-2}, f_{m-1}), \\
0 &= -\mathrm{rem}(f_{m-1}, f_m),
\end{aligned}
$$

where $\mathrm{rem}(f_i, f_{i+1})$ is the remainder of the polynomial long division of f_i by f_{i+1}. The sequence ends at f_m, when f_{m-1} divided by f_m gives a remainder of zero. For a polynomial of degree n, there are $m \leq n+1$ Sturm polynomials in the sequence.

Theorem 1 (Sturm's theorem) *Let $f(x)$ be a real-valued univariate polynomial and $a, b \in \mathbb{R} \cup \{-\infty, +\infty\}$, with $a < b$ and $f(a), f(b) \neq 0$. Then the number of zeroes of $f(x)$ in the interval (a, b) is the difference*

$$var(\mathcal{F}, a) - var(\mathcal{F}, b) \ ,$$

*where $\mathcal{F}$ is the Sturm sequence of $f(x)$, and the **variations** $var(\mathcal{F}, a)$ and $var(\mathcal{F}, b)$ are the number of times that consecutive nonzero elements of the Sturm sequence—evaluated at a and b, respectively—have opposite signs.* (Adapted from [12].)

4.2   Number of steady states and bistability

Our approach involves identifying regions of bistability by finding conditions that lead to three steady states, without requiring numerical determination of the exact values or stability of the equilibrium points.

While it is in general not possible to draw conclusions on the stability properties of equilibria by simply counting their number, the circuits under consideration enjoy two important properties—namely, they are dissipative and their linearizations are positive—that allow us to relate their degree and number of equilibria to the stability properties of each equilibrium (see Supporting Information). For such circuits, when three equilibria are present, two of them must be stable and one must be unstable.

5   Results

5.1   Genetic toggle circuit comparison

A recent study identified a set of eleven *minimal bistable networks* (MBNs), simple two-gene circuits with the capacity for bistability that do not also contain a smaller bistable subcircuit [13]. One of these MBNs, consisting of two mutually-repressing dimeric proteins (Fig. 1A, top), resembles the toggle that was among the very first synthetic biocircuits [14]. Another is a toggle variant in which one of the repressors functions as a monomer (Fig. 1A, bottom). To our knowledge no monomeric repressor yet exists; however, given the protein engineering capabilities of synthetic biology, predicting how such a toggle will perform relative to a more natural functional equivalent is worthwhile. We refer to these two MBNs as the dimer-dimer (DD) and monomer-dimer (MD) toggles, respectively.
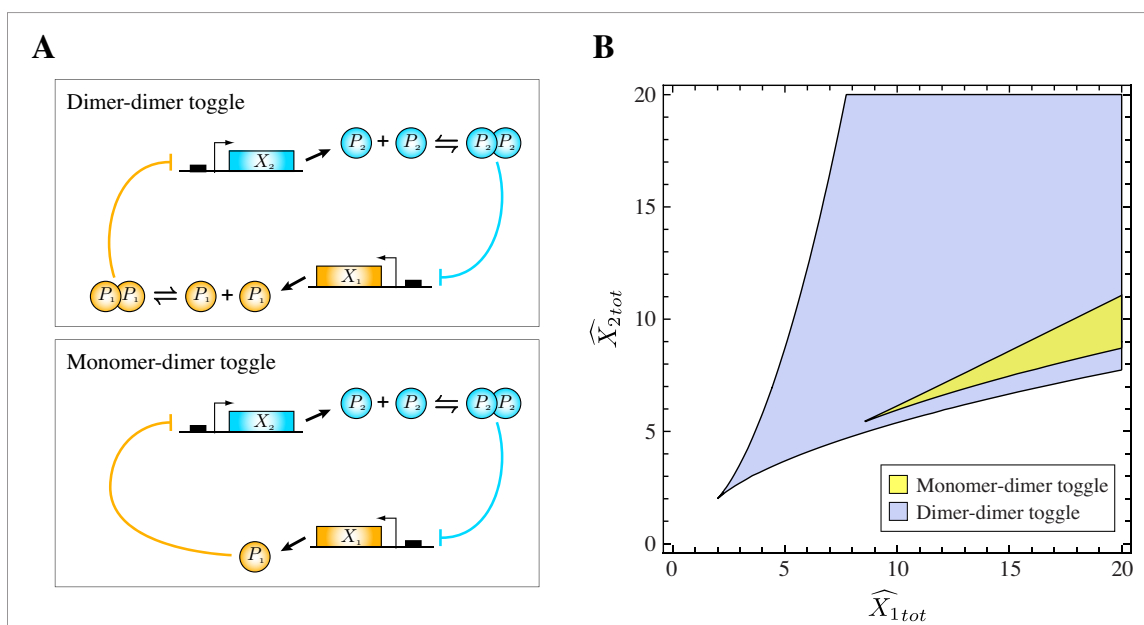

Figure 1: (A) Dimer-dimer (top) and monomer-dimer (bottom) toggle switches. (B) Bistable regions for the monomer-dimer and dimer-dimer toggles.

Beginning with a chemical reaction network formulation and assuming mass-action kinetics we derive ODE models of the two toggles (Eqs. (S1) and (S2)). At equilibrium the concentrations of P_1 and P_2 in the MD system are given by

$$P_{1eq} = \left(1 + (P_{2eq}/K_2)^2\right)^{-1}\beta_1 X_{1tot} , \quad P_{2eq} = \left(1 + (P_{1eq}/K_{md})\right)^{-1}\beta_2 X_{2tot} , \tag{1}$$

and in the DD system,

$$P_{1eq} = \left(1 + (P_{2eq}/K_2)^2\right)^{-1}\beta_1 X_{1tot} , \quad P_{2eq} = \left(1 + (P_{1eq}/K_{dd})^2\right)^{-1}\beta_2 X_{2tot} , \tag{2}$$

where X_{itot} is the total amount of gene i, β_i is the ratio of basal production rate to degradation rate for protein i, and K_{md}, K_{dd}, and K_2 are Michaelis constants (see Supporting Information for details). We may nondimensionalize these equations by scaling the protein concentrations relative to their respective Michaelis constants, and the DNA concentrations accordingly: $\widehat{X}_{2tot} = \beta_2(X_{2tot}/K_2)$, $\widehat{P}_{2eq} = P_{2eq}/K_2$, $\widehat{P}_{1eq} = P_{1eq}/K_{xd}$, and $\widehat{X}_{1tot} = \beta_1(X_{1tot}/K_{xd})$. Systems (1) and (2) can then be written as polynomials in $\widehat{P}_{1eq}$:

$$f_{md}(\widehat{P}_{1eq}) = \widehat{P}_{1eq}^3 - (\widehat{X}_{1tot} - 2)\widehat{P}_{1eq}^2 - (2\widehat{X}_{1tot} - \widehat{X}_{2tot}^2 - 1)\widehat{P}_{1eq} - \widehat{X}_{1tot} = 0 \tag{3}$$

and

$$f_{dd}(\widehat{P}_{1eq}) = \widehat{P}_{1eq}^5 - \widehat{X}_{1tot}\widehat{P}_{1eq}^4 + 2\widehat{P}_{1eq}^3 - 2\widehat{X}_{1tot}\widehat{P}_{1eq}^2 + (\widehat{X}_{2tot}^2 + 1)\widehat{P}_{1eq} - \widehat{X}_{1tot} = 0 \;, \tag{4}$$

for the MD and DD toggles, respectively. Every positive root of these equilibrium polynomials gives a positive steady state concentration for every other circuit component as well. To find the regions of bistability in the plane of $\widehat{X}_{1tot}$ and $\widehat{X}_{2tot}$, we construct the Sturm sequence $\mathcal{F}$ associated with each circuit's equilibrium polynomial (Eq. (3) or (4)), evaluate $\mathcal{F}$ at $\widehat{P}_{1eq} \to 0$ and $\widehat{P}_{1eq} \to +\infty$, and find the conditions leading to a variation difference $var(\mathcal{F}, 0) - var(\mathcal{F}, +\infty) = 3$. (Sturm sequences are given in the Supporting Information.)

The MD toggle Sturm sequence $\mathcal{F}_{md}$ has a maximum possible variation of 3 and only one combination of inequalities that can give rise to bistability: when $var(\mathcal{F}_{md}, 0) = 3$ and $var(\mathcal{F}_{md}, +\infty) = 0$. In contrast, the DD toggle sequence $var(\mathcal{F}_{dd}$ could in principle yield five or four positive steady states; however, only three are admitted as there are no combinations of inequalities that have a variation difference of 5 or 4 and are logically consistent. All possible sign sets for the DD toggle are listed along with their allowabilities in Tables S1 and S2. The analytic expressions for the two regions of bistability are Eq. (S14) (MD toggle) and the intersection of Eqs. (S15) and (S16) (DD toggle). We find that the DD toggle operates over a substantially greater range than the MD toggle (Fig. 1B), indicating that the DD architecture is more functionally robust to variations in circuit DNA concentration (given fixed rate parameters). Furthermore, the DD switch can operate with significantly lower concentrations of DNA: a >50% reduction in $\widehat{X}_{2tot}$ and >75% reduction in $\widehat{X}_{1tot}$.

Recognizing that some of the mathematical tools used may be unfamiliar, some computational validation of our results may be of value. Computational tests and results that perfectly match the Sturm results are described in the Supporting Information.

5.2 Single gene circuit bistability

The single gene system consisting of bacteriophage λ repressor and its promoter P_{RM} (with its three operator sites OR1, OR2, and OR3) also exhibits bistability [15]. We can compare the bistability region of this multi-operator circuit with that of a simple positive feedback circuit containing only one operator site.

A dimensionless model of the λ single gene system is given in [15]. At steady state the concentration of protein is given by

$$\gamma\sigma_1\sigma_2 P_{eq}^7 + \gamma\sigma_1 P_{eq}^5 - \alpha\sigma_1 P_{eq}^4 + \gamma P_{eq}^3 - P_{eq}^2 + \gamma P_{eq} - 1 = 0 \;, \tag{5}$$

where γ is the rescaled degradation rate constant, α represents the increase in protein production resulting from dimer binding to OR2, and σ_1 and σ_2 are the relative (to OR1) affinities for OR2 and the negatively-regulating OR3, respectively. (For simplicity we set the gene copy number equal to one.) With $\sigma_1 = 2$ and

$\sigma_2 = 0.08$ [15], the associated Sturm sequence $\mathcal{F}_{\mathrm{P_{RM}}}$ has only two sign sets with $var(\mathcal{F}_{\mathrm{P_{RM}}}, 0) = 5$ and one set with $var(\mathcal{F}_{\mathrm{P_{RM}}}, +\infty) = 2$ that are logically consistent and together give bistability (Table S3).

In contrast, for a single gene positive feedback system with one operator site for its dimeric protein (MBN *kqw* in [13]), rescaled as in Eq. (5), we have:

$$\gamma P_{eq}^3 - \alpha P_{eq}^2 + \gamma P_{eq} - 1 = 0 \ . \tag{6}$$

As with the MD toggle, this polynomial also has a maximum possible variation of 3 and thus only a single combination of inequalities that give rise to bistability, in the region given by Eq. (S17).

The bistable regions (in α–γ space) for these single gene systems are shown in Fig. 2A. It can be seen that the λ repressor circuit functions over a larger range and with lower values of the degradation rate constant. Interestingly, with $\alpha = 11$ ([15] and references therein) the single operator circuit would only just barely function as a bistable circuit, and any small fluctuation in circuit parameters would render it nonfunctional.
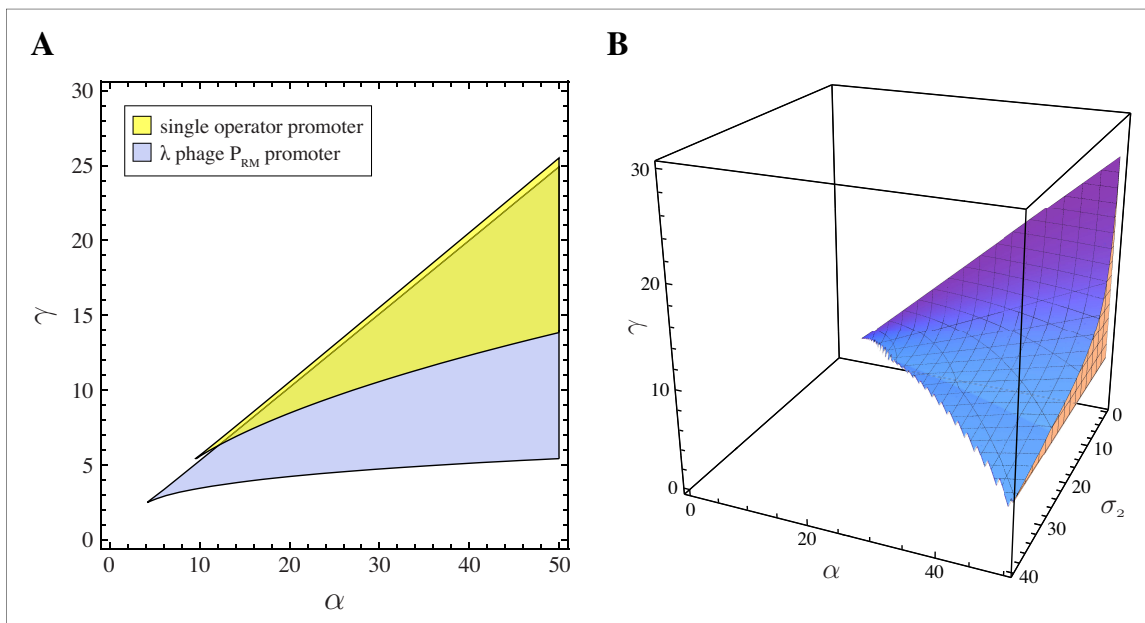

Figure 2: (A) Bistable regions for the single operator positive feedback circuit and the λ repressor–$\mathrm{P_{RM}}$ system with relative affinities $\sigma_1 = 2$ and $\sigma_2 = 0.08$. (B) Region of bistability for the λ–$\mathrm{P_{RM}}$ system as a function of protein production enhancement α, protein degradation rate γ, and relative affinity for OR3 σ_2.

Sturm's theorem may also be used to determine how the strength of the negative feedback (σ_2) affects bistability. Keeping $\sigma_1 = 2$, and using $\alpha = 11$ and $\gamma = 4.5$ (centered in the bistable region at $\alpha = 11$; see Fig. 2A), we find that σ_2 can increase twelve-fold to ~ 0.96 before bistability is lost. In general, significant increases in σ_2 require similar increases in α for bistability to maintained, with the range of allowable γ narrowing as result (Fig. 2B).

6 Discussion

We have shown how real algebraic geometry, specifically Sturm's theorem, can be used to compare and contrast functionally equivalent bistable biocircuits. We take advantage of the fact that the circuits discussed

here, like many in biology, are dissipative and positive in their linearization, which allows us to ascertain the stability of their equilibria without computation. For each circuit the bistability region is given as a set of exact inequalities, simplified by the combination of the (often unknown and fixed) rate parameters into rescaling factors. Though applied to only four different bistable circuits here, this same approach may be used for any system that at steady state can be described by a univariate polynomial.

Comparing two different genetic toggle variants, we see that one consisting of two dimeric repressor species has a wider operational range than one composed of one dimeric and one monomeric repressor. This result demonstrates the general importance of comparing functionally equivalent circuits, with particular relevance for the design of larger circuits that rely on bistable modules: given the uncertainty that exists in parameter values and DNA concentration (when DNA is in the form of plasmids without strict copy-number control), a bistable circuit variant that works over a wide range of parameters would most likely be preferable.

Our results also demonstrate the benefit of an additional operator site for a real single gene positive feedback system: if the λ repressor–P_{RM} system did not have both OR1 and OR2, the enhancement $\alpha = 11$ would barely be sufficient for the system to be bistable. We also see that the negative feedback at OR3 is small enough to not significantly affect bistability. This suggests that the promoter architecture of the λ system may have evolved to allow for both robust bistability due to the positive feedback as well as reduced variability or other benefit of negative autoregulation.

We have used Sturm's theorem to distinguish between biocircuits known to exhibit bistability. However, it may also be used (like Chemical Reaction Network Theory, previously [13, 16]) to predict new bistable topologies or rule out those circuits that do not have this capacity, since only those circuits with a variation difference $var(\mathcal{F}, 0) - var(\mathcal{F}, +\infty) = 3$ for some sets of parameters can be bistable. Altogether the addition of real algebraic geometry to the general synthetic biology toolbox can only help improve the process of biological circuit design and analysis.

7   Acknowledgements

References

[1] Purnick PEM, Weiss R. The second wave of synthetic biology: from modules to systems. Nature Reviews Molecular Cell Biology. 2009;10(6):410–422.

[2] Lim WA, Lee CM, Tang C. Design principles of regulatory networks: searching for the molecular algorithms of the cell. Mol Cell. 2013 Jan;49(2):202–212.

[3] Rouault H, Hakim V. Different cell fates from cell-cell interactions: core architectures of two-cell bistable networks. Biophys J. 2012 Feb;102(3):417–426.

[4] Yao G, Tan C, West M, Nevins JR, You L. Origin of bistability underlying mammalian cell cycle entry. Mol Syst Biol. 2011 Apr;7:485.

[5] Ho KL, Harrington HA. Bistability in apoptosis by receptor clustering. PLoS Comput Biol. 2010;6(10):e1000956.

[6] Tiwari A, Ray JCJ, Narula J, Igoshin OA. Bistable responses in bacterial genetic networks: designs and dynamical consequences. Mathematical Biosciences. 2011 May;231(1):76–89.

[7] Ma W, Trusina A, El-Samad H, Lim WA, Tang C. Defining network topologies that can achieve biochemical adaptation. Cell. 2009 Aug;138(4):760–773.

[8] Blanchini F, Franco E. Structurally robust biological networks. BMC Syst Biol. 2011;5:74.

[9] Blanchini F, Franco E, Giordano G. A structural classification of candidate oscillators and multistationary systems. bioRxiv. 2013;.

[10] Sturm CF. Mémoire sur la résolution des équations numériques. In: Collected Works of Charles François Sturm. Basel: Birkhäuser Basel; 2009. p. 345–390.

[11] Eisermann M. The Fundamental Theorem of Algebra Made Effective: An Elementary Real-algebraic Proof via Sturm Chains. The American Mathematical Monthly. 2012;119(9):715–752.

[12] Sottile F. Real Solutions to Equations from Geometry. American Mathematical Society; 2011.

[13] Siegal-Gaskins D, Mejia-Guerra MK, Smith GD, Grotewold E. Emergence of switch-like behavior in a large family of simple biochemical networks. PLoS Comput Biol. 2011 May;7(5):e1002039.

[14] Gardner TS, Cantor CR, Collins JJ. Construction of a genetic toggle switch in Escherichia coli. Nature. 2000 Jan;403(6767):339–342.

[15] Hasty J, Isaacs F, Dolnik M, McMillen D, Collins JJ. Designer gene networks: Towards fundamental cellular control. Chaos. 2001 Feb;11(1):207–220.

[16] Siegal-Gaskins D, Grotewold E, Smith GD. The capacity for multistability in small gene regulatory networks. BMC Syst Biol. 2009;3:96.
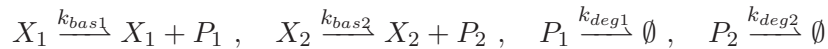
An analytical approach to bistable biological circuit discrimination using real algebraic geometry:
Supporting Information

Dan Siegal-Gaskins[1], Elisa Franco[2], Tiffany Zhou[1], and Richard M. Murray[1,3]
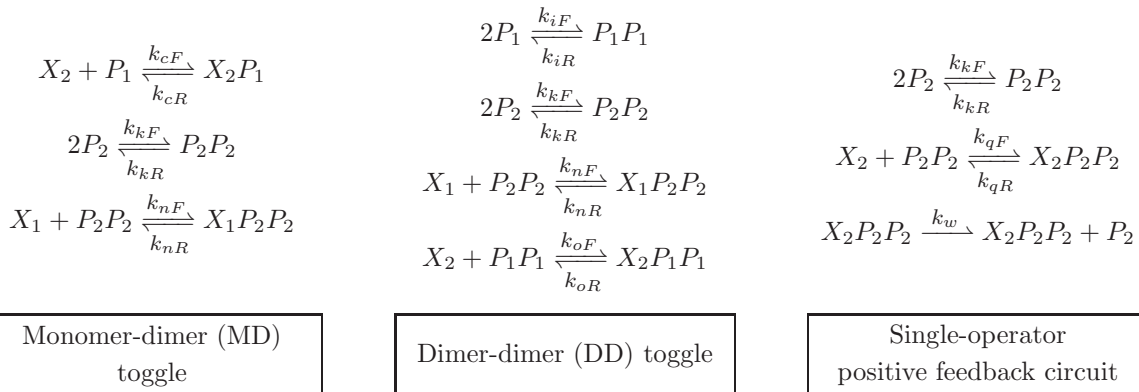
1. Division of Biology and Biological Engineering, California Institute of Technology, Pasadena, CA, USA
2. Department of Mechanical Engineering, University of California at Riverside, Riverside, CA, USA
3. Department of Control and Dynamical Systems, California Institute of Technology, Pasadena, CA, USA

1   Chemical reaction networks

With the exception of the model for the multiple-operator P_{RM} promoter of bacteriophage λ, the various circuits highlighted in the main text were initially predicted to exhibit bistability using a chemical reaction network (CRN)-based topological survey [1]. Each of these CRNs contains reactions representing basal protein production and degradation:

$$X_1 \xrightarrow{k_{bas1}} X_1 + P_1 \ , \quad X_2 \xrightarrow{k_{bas2}} X_2 + P_2 \ , \quad P_1 \xrightarrow{k_{deg1}} \emptyset \ , \quad P_2 \xrightarrow{k_{deg2}} \emptyset$$

for genes X_i and proteins P_i. The other reactions that uniquely define each circuit are:

$$X_2 + P_1 \underset{k_{cR}}{\overset{k_{cF}}{\rightleftharpoons}} X_2 P_1$$

$$2P_2 \underset{k_{kR}}{\overset{k_{kF}}{\rightleftharpoons}} P_2 P_2$$

$$X_1 + P_2 P_2 \underset{k_{nR}}{\overset{k_{nF}}{\rightleftharpoons}} X_1 P_2 P_2$$

Monomer-dimer (MD) toggle

$$2P_1 \underset{k_{iR}}{\overset{k_{iF}}{\rightleftharpoons}} P_1 P_1$$

$$2P_2 \underset{k_{kR}}{\overset{k_{kF}}{\rightleftharpoons}} P_2 P_2$$

$$X_1 + P_2 P_2 \underset{k_{nR}}{\overset{k_{nF}}{\rightleftharpoons}} X_1 P_2 P_2$$

$$X_2 + P_1 P_1 \underset{k_{oR}}{\overset{k_{oF}}{\rightleftharpoons}} X_2 P_1 P_1$$

Dimer-dimer (DD) toggle

$$2P_2 \underset{k_{kR}}{\overset{k_{kF}}{\rightleftharpoons}} P_2 P_2$$

$$X_2 + P_2 P_2 \underset{k_{qR}}{\overset{k_{qF}}{\rightleftharpoons}} X_2 P_2 P_2$$

$$X_2 P_2 P_2 \xrightarrow{k_w} X_2 P_2 P_2 + P_2$$

Single-operator positive feedback circuit

$P_i P_i$ represent dimeric species, and $X_i P_j$ and $X_i P_j P_j$ represent monomers and dimers bound to the gene promoters. The various ODE sets were derived from these CRNs under the assumption of mass action kinetics and simplified using the fact that the total concentrations of each gene (in bound and unbound form) are conserved.

2 Ordinary differential equation models

From the chemical reaction network formulation and assuming mass-action kinetics we can derive the following sets of ordinary differential equations (ODEs) that describe the circuit dynamics. For the MD toggle:

$$P_1{}'(t) = -k_{deg1}P_1(t) - k_{cF}X_2(t){\cdot}P_1(t) + k_{bas1}X_1(t) + k_{cR}(X_{2tot} - X_2(t)) \tag{S1a}$$

$$P_2{}'(t) = -2k_{kF}P_2(t)^2 - k_{deg2}P_2(t) + 2k_{kR}P_2P_2(t) + k_{bas2}X_2(t) \tag{S1b}$$

$$P_2P_2{}'(t) = k_{kF}P_2(t)^2 - k_{kR}P_2P_2(t) - k_{nF}P_2P_2(t){\cdot}X_1(t) + k_{nR}(X_{1tot} - X_1(t)) \tag{S1c}$$

$$X_1{}'(t) = k_{nR}(X_{1tot} - X_1(t)) - k_{nF}P_2P_2(t){\cdot}X_1(t) \tag{S1d}$$

$$X_2{}'(t) = k_{cR}(X_{2tot} - X_2(t)) - k_{cF}P_1(t){\cdot}X_2(t) \ , \tag{S1e}$$

the DD toggle:

$$P_1{}'(t) = -2k_{iF}P_1(t)^2 - k_{deg1}P_1(t) + 2k_{iR}P_1P_1(t) + k_{bas1}X_1(t) \tag{S2a}$$

$$P_1P_1{}'(t) = k_{iF}P_1(t)^2 - k_{iR}P_1P_1(t) - k_{oF}P_1P_1(t){\cdot}X_2(t) + k_{oR}(X_{2tot} - X_2(t)) \tag{S2b}$$

$$P_2{}'(t) = -2k_{kF}P_2(t)^2 - k_{deg2}P_2(t) + 2k_{kR}P_2P_2(t) + k_{bas2}X_2(t) \tag{S2c}$$

$$P_2P_2{}'(t) = k_{kF}P_2(t)^2 - k_{kR}P_2P_2(t) - k_{nF}P_2P_2(t){\cdot}X_1(t) + k_{nR}(X_{1tot} - X_1(t)) \tag{S2d}$$

$$X_1{}'(t) = k_{nR}(X_{1tot} - X_1(t)) - k_{nF}P_2P_2(t){\cdot}X_1(t) \tag{S2e}$$

$$X_2{}'(t) = k_{oR}(X_{2tot} - X_2(t)) - k_{oF}P_1P_1(t){\cdot}X_2(t) \ , \tag{S2f}$$

and single-operator positive feedback circuit:

$$P_2{}'(t) = k_{bas2}X_2(t) - k_{deg2}P_2(t) - 2k_{kF}P_2(t)^2 + 2k_{kR}P_2P_2(t) + k_w(X_{2tot} - X_2(t)) \tag{S3a}$$

$$P_2P_2{}'(t) = k_{kF}P_2(t)^2 - k_{kR}P_2P_2(t) - k_{qF}P_2P_2(t){\cdot}X_2(t) + k_{qR}(X_{2tot} - X_2(t)) \tag{S3b}$$

$$X_2{}'(t) = k_{qR}(X_{2tot} - X_2(t)) - k_{qF}P_2P_2(t){\cdot}X_2(t) \ , \tag{S3c}$$

where the variable names are as in [1]: X_i is the concentration of free (i.e., unbound by repressor) gene i, X_{itot} is the total amount of X_i in the circuit (bound and unbound), and P_i and P_iP_i represent the monomeric and dimeric forms of protein i, respectively. The various k_x are the reaction rates, and in the positive feedback circuit, $k_w > k_{bas2}$ is assumed.

3 Derivation of the toggle circuit equilibrium polynomials

Using (S1) and (S2), with the left-hand sides set equal to zero, we can derive the univariate equilibrium polynomials used in the application of Sturm's theorem.

For the DD toggle, we subtract (S2d) from (S2e):

$$0 = k_{nR}(X_{1tot} - X_1) - k_{nF}P_2P_2{\cdot}X_1$$

$$- k_{kF}P_2^2 + k_{kR}P_2P_2 + k_{nF}P_2P_2{\cdot}X_1 - k_{nR}(X_{1tot} - X_1)$$

$$\implies P_2P_2 = \frac{k_{kF}}{k_{kR}}P_2^2 = \frac{P_2^2}{k_{kD}} \ , \tag{S4}$$

where for simplicity of notation we use X_i, P_i, and P_iP_i to mean the equilibrium concentrations. We then plug this expression into (S2e) to get

$$0 = k_{nR}(X_{1tot} - X_1) - k_{nF}(P_2^2/k_{kD}){\cdot}X_1$$

$$= (X_{1tot} - X_1) - (P_2^2/(k_{kD}k_{nD})){\cdot}X_1$$

$$\implies X_1 = \frac{k_{kD}k_{nD}X_{1tot}}{k_{kD}k_{nD} + P_2^2} \ . \tag{S5}$$

Similarly we subtract (S2b) from (S2f)

$$0 = k_{oR}(X_{2tot} - X_2) - k_{oF}P_1P_1 \cdot X_2$$
$$- k_{iF}P_1^2 + k_{iR}P_1P_1 + k_{oF}P_1P_1 \cdot X_2 - k_{oR}(X_{2tot} - X_2)$$
$$\implies P_1P_1 = \frac{k_{iF}}{k_{iR}}P_1^2 = \frac{P_1^2}{k_{iD}} \tag{S6}$$

and plug the resulting expression back into (S2f) to get

$$0 = k_{oR}(X_{2tot} - X_2) - k_{oF}(P_1^2/k_{iD}) \cdot X_2$$
$$= (X_{2tot} - X_2) - (P_1^2/(k_{iD}k_{oD})) \cdot X_2$$
$$\implies X_2 = \frac{k_{iD}k_{oD}X_{2tot}}{k_{iD}k_{oD} + P_1^2} \ . \tag{S7}$$

Substituting (S5) and (S7) into (S2a) and (S2c) gives the equilibrium concentrations of P_1 and P_2 in the DD toggle shown in the main text:

$$P_{1eq} = \left(1 + (P_{2eq}/K_2)^2\right)^{-1}\beta_1 X_{1tot} \ , \quad P_{2eq} = \left(1 + (P_{1eq}/K_{dd})^2\right)^{-1}\beta_2 X_{2tot} \ , \tag{S8}$$

where $\beta_i = k_{basi}/k_{degi}$ is the ratio of basal production rate to degradation rate for protein i, and the Michaelis constants $K_{dd} = (k_{iD}k_{oD})^{1/2}$ and $K_2 = (k_{kD}k_{nD})^{1/2}$ represent the protein concentrations that yield 50% of the maximum production rate of their respective targets. The combination of these two expressions gives the DD equilibrium polynomial.

For the MD toggle, we have again that

$$P_2P_2 = \frac{P_2^2}{k_{kD}} \tag{S9}$$

and

$$X_1 = \frac{k_{kD}k_{nD}X_{1tot}}{k_{kD}k_{nD} + P_2^2} \ , \tag{S10}$$

but also (from Eq. (S1e)) that

$$X_2 = \frac{k_{cD}X_{2tot}}{k_{cD} + P_1} \ . \tag{S11}$$

Substituting (S10) and (S11) into (S1a) and (S1b) gives the equilibrium concentrations of P_1 and P_2 in the MD toggle shown in the main text:

$$P_{1eq} = \left(1 + (P_{2eq}/K_2)^2\right)^{-1}\beta_1 X_{1tot} \ , \quad P_{2eq} = \left(1 + (P_{1eq}/K_{md})\right)^{-1}\beta_2 X_{2tot} \ . \tag{S12}$$

As previously, β_i is the ratio of basal production rate to degradation rate for protein i, and the Michaelis constants $K_{md} = k_{cD}$ and $K_2 = (k_{kD}k_{nD})^{1/2}$ represent the protein concentrations that yield 50% of the maximum production rate of their respective targets. The combination of these two expressions gives the MD equilibrium polynomial.

4 Sturm polynomials

Sturm polynomials can be rather long and complicated functions; however, they can be easily generated using software capable of symbolic manipulation, e.g., Mathematica. We present here the Sturm sequences for the MD toggle, DD toggle, and single-operator positive feedback circuit. For simplicity of notation we have used x as our variable in the Sturm polynomials below, rather than the $\widehat{P}_{1eq}$ used in the main text.

The Sturm polynomials associated with the MD toggle equilibrium polynomial are:

$$f_0(x) = (x - \widehat{X}_{1tot})(x+1)^2 + x\widehat{X}_{2tot}^2$$

$$f_1(x) = \widehat{X}_{2tot}^2 + (x+1)(3x - 2\widehat{X}_{1tot} + 1)$$

$$f_2(x) = \frac{1}{9}\left(2(x+1)(\widehat{X}_{1tot}+1)^2 - (6x + \widehat{X}_{1tot} - 2)\widehat{X}_{2tot}^2\right)$$

$$f_3(x) = \frac{9\widehat{X}_{2tot}^2\left(-4\widehat{X}_{2tot}^4 + (\widehat{X}_{1tot}(\widehat{X}_{1tot}+20)-8)\widehat{X}_{2tot}^2 - 4(\widehat{X}_{1tot}+1)^3\right)}{4\left((\widehat{X}_{1tot}+1)^2 - 3\widehat{X}_{2tot}^2\right)^2} \; .$$

The DD Sturm polynomials are:

$$f_0(x) = (x^2+1)^2(x - \widehat{X}_{1tot}) + x\widehat{X}_{2tot}^2$$

$$f_1(x) = (x^2+1)(5x^2 - 4x\widehat{X}_{1tot} + 1) + \widehat{X}_{2tot}^2$$

$$f_2(x) = \frac{1}{25}\left(4(x^2+1)\left(x(\widehat{X}_{1tot}^2 - 5) + 6\widehat{X}_{1tot}\right) - \widehat{X}_{2tot}^2(20x + \widehat{X}_{1tot})\right)$$

$$f_3(x) = \frac{1}{q_3}\left(\widehat{X}_{2tot}^2\left(2\widehat{X}_{1tot}^2 - 4 + 4x^2(\widehat{X}_{1tot}^2 - 5) - 3x\widehat{X}_{1tot}(3 + \widehat{X}_{1tot}^2)\right) - 4(x^2+1)(\widehat{X}_{1tot}^2+1)^2\right)$$

$$f_4(x) = \frac{1}{q_4}4(\widehat{X}_{1tot}^2 - 5)^2\widehat{X}_{2tot}^6(20x + \widehat{X}_{1tot}) - (\widehat{X}_{1tot}^2 - 5)^2\widehat{X}_{2tot}^4\left(x(9\widehat{X}_{1tot}^4 + 35\widehat{X}_{1tot}^2 - 64) - 2\widehat{X}_{1tot}(\widehat{X}_{1tot}^2 - 62)\right)$$

$$+ 16(\widehat{X}_{1tot}^4 - 4\widehat{X}_{1tot}^2 - 5)^2\widehat{X}_{2tot}^2(\widehat{X}_{1tot} - x)$$

$$f_5(x) = \frac{1}{q_5}\left(256\widehat{X}_{1tot}^6 - 3\widehat{X}_{1tot}^4(9\widehat{X}_{2tot}^4 + 32\widehat{X}_{2tot}^2 - 256) - 96\widehat{X}_{1tot}^2(\widehat{X}_{2tot}^4 + 29\widehat{X}_{2tot}^2 - 8) + 256(\widehat{X}_{2tot}^2 + 1)^3\right)$$

$$\times 25\left((\widehat{X}_{1tot}^2 + 1)^2 + (\widehat{X}_{1tot}^2 - 5)\widehat{X}_{2tot}^2\right)^2$$

where

$$q_3 = \frac{4}{25}(\widehat{X}_{1tot}^2 - 5)^2$$

$$q_4 = 100\left((\widehat{X}_{1tot}^2 - 5)\widehat{X}_{2tot}^2 + (\widehat{X}_{1tot}^2 + 1)^2\right)^2$$

$$q_5 = (\widehat{X}_{1tot}^2 - 5)^2\left(16(\widehat{X}_{1tot}^2 + 1)^2 + (9\widehat{X}_{1tot}^4 + 35\widehat{X}_{1tot}^2 - 64)\widehat{X}_{2tot}^2 - 80\widehat{X}_{2tot}^4\right)^2 .$$

For all values of $\widehat{X}_{1tot} \neq \sqrt{5}$, the sequence consisting of the $f_i(x)$ above may be used to determine the number of steady states. However, when $\widehat{X}_{1tot} \to \sqrt{5}$, the sequence terminates prematurely (since $f_4(x) \to 0$) and there are problematic zeros in the denominators of $f_3(x)$ and $f_5(x)$. We thus set $\widehat{X}_{1tot} = \sqrt{5}$ in the equilibrium polynomial to get

$$\widehat{P}_{1eq}^5 - \sqrt{5}\widehat{P}_{1eq}^4 + 2\widehat{P}_{1eq}^3 - 2\sqrt{5}\widehat{P}_{1eq}^2 + \widehat{P}_{1eq}\widehat{X}_{2tot}^2 + \widehat{P}_{1eq} - \sqrt{5} = 0 \; , \tag{S13}$$

and generate a second Sturm sequence to use at $\widehat{X_{1tot}} = \sqrt{5}$ only:

$$f_0(x) = x^5 - \sqrt{5}x^4 + 2x^3 - 2\sqrt{5}x^2 + x\widehat{X}_{2tot}^2 + x - \sqrt{5}$$

$$f_1(x) = 5x^4 - 4\sqrt{5}x^3 + 6x^2 - 4\sqrt{5}x + \widehat{X}_{2tot}^2 + 1$$

$$f_2(x) = \frac{1}{25}\left(24\sqrt{5}x^2 - 20x\widehat{X}_{2tot}^2 - \sqrt{5}\widehat{X}_{2tot}^2 + 24\sqrt{5}\right)$$

$$f_3(x) = -\frac{5}{1728}\left(40\sqrt{5}x\widehat{X}_{2tot}^6 - 168\sqrt{5}x\widehat{X}_{2tot}^4 - 288\sqrt{5}x\widehat{X}_{2tot}^2 + 10\widehat{X}_{2tot}^6 - 285\widehat{X}_{2tot}^4 + 1440\widehat{X}_{2tot}^2\right)$$

$$f_4(x) = -\frac{27(256\widehat{X}_{2tot}^6 - 387\widehat{X}_{2tot}^4 - 15552\widehat{X}_{2tot}^2 + 55296)}{40\sqrt{5}\left(5\widehat{X}_{2tot}^4 - 21\widehat{X}_{2tot}^2 - 36\right)^2} \ .$$

The single-operator positive feedback circuit Sturm sequence contains the following polynomials:

$$f_0(x) = \alpha x^2 - \gamma\left(x^3 + x\right) + 1$$

$$f_1(x) = 2\alpha x - \gamma\left(3x^2 + 1\right)$$

$$f_2(x) = \frac{1}{9}\left(-\frac{2\alpha^2 x}{\gamma} + \alpha + 6\gamma x - 9\right)$$

$$f_3(x) = \frac{9\gamma\left(4\alpha^3 - \alpha^2\gamma^2 - 18\alpha\gamma^2 + 4\gamma^4 + 27\gamma^2\right)}{4\left(\alpha^2 - 3\gamma^2\right)^2} \ .$$

Recall that γ is the rescaled degradation rate constant for the λ repressor and α represents the increase in protein production resulting from repressor dimer binding to OR2.

5   Sturm sequence sign combinations

We list in the tables below the various possible sets of Sturm sequence inequalities for the DD toggle (Tables S1 and S2) and λ repressor–P_{RM} system (Tables S3). (The MD toggle and single-operator positive feedback circuit each have only one combination of inequalities that can give rise to bistability.) The inequality sets are written in compact form as $\{\pm \pm \cdots \pm\}$. 'Allowed' refers to the logical consistency of the inequality set (i.e., whether all inequalities can be simultaneously satisfied) and was determined using Mathematica. For simplicity of notation in the tables we only show $+$ and $-$ in the various sequence positions, even though there are cases where a particular Sturm polynomial may be equal to zero without affecting the total number of sign changes; for example, for the DD toggle, both $\{-+--+-\}$ and $\{-+0-+-\}$ give a variation of 4. (Recall that Sturm's theorem is only concerned with consecutive nonzero elements and zeros are ignored.) When zeros were valid options for the sequence, otherwise strict inequalities were made nonstrict (e.g., '$>$' $\to$ '$\geq$').

6

$var(\mathcal{F}_{dd},0)$	$sign(\mathcal{F}_{dd},0)$	Allowed?	$var(\mathcal{F}_{dd},+\infty)$	$sign(\mathcal{F}_{dd},+\infty)$	Allowed?
5	$\{-+-+-+\}$	N	2	$\vdots$	$\vdots$
4	$\{-+-+--\}$ $\{-+--+-\}$ $\{-++-+-\}$ $\{-+-++-\}$	N Y Y Y	1	$\{+++++-\}$ $\{++++--\}$ $\{+++---\}$ $\{++----\}$	N N Y Y
3	$\vdots$	$\vdots$	0	$\{++++++\}$	N

Table S1: Sturm sequence inequality sets for the DD toggle when $\widehat{X}_{1tot} \neq \sqrt{5}$. The signs of the first two polynomials are fixed at $\widehat{P}_{1eq} \to 0$ and $\widehat{P}_{1eq} \to +\infty$. Neither $var(\mathcal{F}_{dd},0) = 5$ nor $var(\mathcal{F}_{dd},+\infty) = 0$ represent logically consistent sets, eliminating the need to consider any sets that could in theory satisfy $var(\mathcal{F}_{dd},+\infty) = 2$ or $var(\mathcal{F}_{dd},0) = 3$ as candidates for bistability.

$var(\mathcal{F}_{dd},0)$	$sign(\mathcal{F}_{dd},0)$	Allowed?	$var(\mathcal{F}_{dd},+\infty)$	$sign(\mathcal{F}_{dd},+\infty)$	Allowed?
4	$\{-+-+-\}$	N	1	$\vdots$	$\vdots$
3	$\{-+-++\}$ $\{-++-+\}$ $\{-+--+\}$	N Y N	0	$\{+++++\}$	Y

Table S2: Sturm sequence inequality sets for the DD toggle when $\widehat{X}_{1tot} = \sqrt{5}$. The signs of the first two and three polynomials are fixed at $\widehat{P}_{1eq} \to 0$ and $\widehat{P}_{1eq} \to +\infty$, respectively. The set with $var(\mathcal{F}_{dd},0) = 4$ is not logically consistent, eliminating the need to consider any sets that could in theory satisfy $var(\mathcal{F}_{dd},+\infty) = 1$ as candidates for bistability.

$var(\mathcal{F}_{\mathrm{P_{RM}}},0)$	$sign(\mathcal{F}_{\mathrm{P_{RM}}},0)$	Allowed?	$var(\mathcal{F}_{\mathrm{P_{RM}}},+\infty)$	$sign(\mathcal{F}_{\mathrm{P_{RM}}},+\infty)$	Allowed?
6	$\{-++-+-+-\}$	N	3	$\vdots$	$\vdots$
5	$\{-++-+-++\}$ $\{-++-++-+\}$ $\{-++-+--+\}$ $\{-++--+-+\}$	N Y N Y	2	$\{++--++++\}$ $\{++---+++\}$ $\{++-----++\}$ $\{++------+\}$	N Y N N
4	$\vdots$	$\vdots$	1	$\{++------\}$	N

Table S3: Sturm sequence inequality sets for the λ repressor–$\mathrm{P_{RM}}$ system. The first four Sturm polynomials have fixed signs at $P_{eq} = 0$ and $P_{eq} = +\infty$. Neither $var(\mathcal{F}_{\mathrm{P_{RM}}},0) = 6$ nor $var(\mathcal{F}_{\mathrm{P_{RM}}},+\infty) = 1$ represent logically consistent sets, eliminating the need to consider any sets that could in theory satisfy $var(\mathcal{F}_{\mathrm{P_{RM}}},+\infty) = 3$ or $var(\mathcal{F}_{\mathrm{P_{RM}}},0) = 4$ as candidates for bistability.

6 Analytic expressions for regions of bistability

The regions of bistability were determined by combining the valid inequality sets and reducing to a single pair of inequalities in the plane of the relevant variables. Reduction was done using Mathematica.

There is only one combination of inequalities that can give rise to bistability for the MD toggle: when $var(\mathcal{F}_{md}, 0) = 3$ and $var(\mathcal{F}_{md}, +\infty) = 0$. This gives the region of bistability in $\widehat{X}_{1tot}$–$\widehat{X}_{2tot}$ space as

$$\widehat{X}_{1tot} > 8$$
$$\frac{1}{8}\left(20\widehat{X}_{1tot} + \widehat{X}_{1tot}^2 - 8 - f(\widehat{X}_{1tot})\right) \le \widehat{X}_{2tot}^2 \le \frac{1}{8}\left(20\widehat{X}_{1tot} + \widehat{X}_{1tot}^2 - 8 + f(\widehat{X}_{1tot})\right), \tag{S14}$$

with $f(\widehat{X}_{1tot}) = (\widehat{X}_{1tot} - 8)^{3/2}(\widehat{X}_{1tot})^{1/2}$.

In the case of the DD toggle, there are two different Sturm sequences we need to consider depending on the value of $\widehat{X}_{1tot}$ (see Section 'Sturm polynomials' above). When $\widehat{X}_{1tot} \ne \sqrt{5}$, the Sturm sequence $\mathcal{F}_{dd}$ contains six polynomials, and there are three sets of inequalities with $var(\mathcal{F}_{dd}, 0) = 4$ and two with $var(\mathcal{F}_{dd}, +\infty) = 1$ that are logically consistent (Table S1). When $\widehat{X}_{1tot} = \sqrt{5}$, the sequence $\mathcal{F}_{dd}$ contains five polynomials, and only one set of inequalities with $var(\mathcal{F}_{dd}, 0) = 3$ and one with $var(\mathcal{F}_{dd}, +\infty) = 0$ are allowed (Table S2). These inequalities may be combined to give a continuous region of bistability as the intersection of

$$\widehat{X}_{1tot} > 4$$
$$0 < \widehat{X}_{2tot}^2 \le \frac{1}{160}\left(9\widehat{X}_{1tot}^4 + 35\widehat{X}_{1tot}^2 - 64 + 3\left(9\widehat{X}_{1tot}^8 + 70\widehat{X}_{1tot}^6 + 577\widehat{X}_{1tot}^4 + 640\widehat{X}_{1tot}^2 + 1024\right)^{1/2}\right) \tag{S15}$$

and

$$256\left(\widehat{X}_{1tot}^6 + (\widehat{X}_{2tot}^2 + 1)^3\right) < 3\widehat{X}_{1tot}^4\left(9\widehat{X}_{2tot}^4 + 32\widehat{X}_{2tot}^2 - 256\right) + 96\widehat{X}_{1tot}^2\left(\widehat{X}_{2tot}^4 + 29\widehat{X}_{2tot}^2 - 8\right). \tag{S16}$$

As with the MD toggle, the equilibrium polynomial for the single-operator positive feedback circuit also has a maximum possible variation of 3, which means that the circuit exhibits bistability only in the region

$$\alpha > 9$$
$$\frac{1}{8}\left(\alpha^2 + 18\alpha - 27 - (\alpha - 9)^{3/2}(\alpha - 1)^{1/2}\right) \le \gamma^2 \le \frac{1}{8}\left(\alpha^2 + 18\alpha - 27 + (\alpha - 9)^{3/2}(\alpha - 1)^{1/2}\right). \tag{S17}$$

With the exception of the DD toggle at $\widehat{X}_{1tot} = \sqrt{5}$ (which was treated by analyzing a second Sturm sequence; see 'Sturm polynomials' section above), none of the potential zeroes in the Sturm polynomial denominators required special treatment nor did they present any problems in determining the regions of bistability.

7 Circuit Jacobians

The Jacobian matrices for the MD toggle, DD toggle, and single-operator positive feedback circuit are:

$$J_{md} = \begin{pmatrix} -k_{deg1} - k_{cF}X_2(t) & 0 & 0 & k_{bas1} & -k_{cR} - k_{cF}P_1(t) \\ 0 & -k_{deg2} - 4k_{kF}P_2(t) & 2k_{kR} & 0 & k_{bas2} \\ 0 & 2k_{kF}P_2(t) & -k_{kR} - k_{nF}X_1(t) & -k_{nR} - k_{nF}P_2P_2(t) & 0 \\ 0 & 0 & -k_{nF}X_1(t) & -k_{nR} - k_{nF}P_2P_2(t) & 0 \\ -k_{cF}X_2(t) & 0 & 0 & 0 & -k_{cR} - k_{cF}P_1(t) \end{pmatrix} \tag{S18}$$

$$J_{dd} = \begin{pmatrix} -k_{deg1}-4k_{iF}P_1(t) & 2k_{iR} & 0 & 0 & k_{bas1} & 0 \\ 2k_{iF}P_1(t) & -k_{iR}-k_{oF}X_2(t) & 0 & 0 & 0 & -k_{oR}-k_{oF}P_1P_1(t) \\ 0 & 0 & -k_{deg2}-4k_{kF}P_2(t) & 2k_{kR} & 0 & k_{bas2} \\ 0 & 0 & 2k_{kF}P_2(t) & -k_{kR}-k_{nF}X_1(t) & -k_{nR}-k_{nF}P_2P_2(t) & 0 \\ 0 & 0 & 0 & -k_{nF}X_1(t) & -k_{nR}-k_{nF}P_2P_2(t) & 0 \\ 0 & -k_{oF}X_2(t) & 0 & 0 & 0 & -k_{oR}-k_{oF}P_1P_1(t) \end{pmatrix} \quad \text{(S19)}$$

$$J_{pf} = \begin{pmatrix} -k_{deg2} - 4k_{kF}P_2(t) & 2k_{kR} & k_{bas2} - k_w \\ 2k_{kF}P_2(t) & -k_{kR} - k_{qF}X_2(t) & -k_{qR} - k_{qF}P_2P_2(t) \\ 0 & -k_{qF}X_2(t) & -k_{qR} - k_{qF}P_2P_2(t) \end{pmatrix} \quad \text{(S20)}$$

Each of the Jacobian matrices J may be transformed to Metzler matrices J_M with a similarity transformation: $J_M = P^{-1}JP$. (The P matrices for the MD toggle, DD toggle, and single-operator positive feedback circuit Jacobians are $P_{md} = \text{diag}(-1, 1, 1, -1, 1)$, $P_{dd} = \text{diag}(-1, -1, 1, 1, -1, 1)$, and $P_{pf} = \text{diag}(1, 1, -1)$, respectively.) The Jacobians are also row equivalent to the identity matrix (as confirmed with Mathematica) and thus invertible—$\det(J) \neq 0$ for all (positive) parameters and equilibria.

8 Number of steady states and stability analysis

8.1 Preliminaries

Definition 1 (Positive systems) *A linear system $\dot{x} = Ax$ is positive if for every nonnegative initial state the solution $x(t)$ is nonnegative.*

The following is a well known condition for positivity [2]:

Theorem 1 *A linear system $\dot{x} = Ax$ is positive if and only if matrix A is a Metzler matrix, i.e., its elements satisfy: $a_{ij} \geq 0, \forall(i, j)$ such that $i \neq j$.*

Since the Jacobian matrices (shown above) are, for any choice of parameters, similar to Metzler matrices via linear transformations, the linearizations of systems (S1), (S2), and (S3) are positive.

The general definition of *dissipativity* (see, e.g., [3]) is based on the existence of compact, forward invariant subsets of $\mathbb{R}^n_+$ that absorb the system trajectories. The following definition (from [4]) is equivalent and easier to verify:

Definition 2 (Dissipative systems) *A system $\dot{x} = f(x)$ is dissipative if its solutions are eventually uniformly bounded, i.e., there exists a constant $k > 0$ such that:*

$$\lim_{t \to +\infty} \sup x_i(t) \leq k.$$

Systems (S1), (S2), and (S3) are dissipative. As an example, we verify the definition for the MD toggle model (S1). Because the total mass of each of the DNA species X_1 and X_2 is constant, we know that $X_1(t) \leq X_{max}$ and $X_2(t) \leq X_{max}$ $\forall t$, where $X_{max} = \max\{X_{1tot}, X_{2tot}\}$. The dynamics of P_1 can be upper bounded as follows:

$$\begin{aligned} P_1{}'(t) &= -k_{deg1}P_1(t) - k_{cF}X_2(t)P_1(t) + k_{bas1}X_1(t) + k_{cR}(X_{2tot} - X_2(t)) \\ &\leq -k_{deg1}P_1(t) - k_{cF}X_{max}P_1(t) + k_{bas1}X_{max} + k_{cR}X_{max} \\ &\leq -aP_1(t) + b, \end{aligned}$$

where $a = k_{deg1} + k_{cF}X_{max}$ and $b = k_{bas1}X_{max} + k_{cR}X_{max}$. The right hand side of the last inequality above is a linear, asymptotically stable system whose solution is eventually uniformly bounded (b is a finite constant). Using the comparison principle [5], we conclude that $P_1(t)$ is bounded and can find a constant k that satisfies the definition.

As for P_2 and its dimer, we know that $P_{2tot}(t) = P_2P_2(t) + P_2(t)$, thus $P_2(t) \leq P_{2tot}(t)$ and $P_2P_2(t) \leq P_{2tot}(t)$. Therefore we only need to show that $P_{2tot}(t)$ is eventually uniformly bounded. We have that

$$\begin{aligned}
P_{2tot}{}'(t) &= P_2{}'(t) + 2P_2P_2{}'(t) \\
&= -2k_{kF}P_2(t)^2 - k_{deg2}P_2(t) + 2k_{kR}P_2P_2(t) + k_{bas2}X_2(t) \\
&\quad + 2k_{kF}P_2(t)^2 - 2k_{kR}P_2P_2(t) - 2k_{nF}P_2P_2(t)X_1(t) + 2k_{nR}(X_{1tot} - X_1(t)) \\
&= k_{bas2}X_2(t) - k_{deg2}P_2(t) - 2k_{nF}P_2P_2(t)X_1(t) + 2k_{nR}(X_{1tot} - X_1(t)) \\
&\leq X_{max}(k_{bas2} + 2k_{nR}) - k_{deg2}P_2(t) - 2k_{nF}X_{max}P_2P_2(t) \\
&\leq c - dP_2{}^{tot} ,
\end{aligned}$$

where $c = X_{max}(k_{bas2} + 2k_{nR})$ and $d = \min\{k_{deg2}, 2k_{nF}X_{max}\}$. Because the dynamics of P_{2tot} are bounded by the dynamics of an asymptotically stable linear system with bounded input c, we conclude that both the monomer and dimer species are eventually uniformly bounded.

The ODE model of the MD toggle system is thus dissipative. Similar proofs can be provided for systems (S2) and (S3).

8.2 Stability of equilibria

Sturm's theorem applied to the polynomial equilibrium conditions for systems (S1), (S2), and (S3) reveals that each system admits three positive equilibria. The stability properties of these equilibria can be determined by *degree theory* [4].

Definition 3 (Regular equilibrium) *An equilibrium point $\bar{x}$ of system $\dot{x} = f(x)$ is regular if $\det(J(\bar{x})) \neq 0$ (in other words, $J(\bar{x})$ must be invertible; alternatively, $J(\bar{x})$ must not have eigenvalues at the origin).*

Definition 4 (Index of an equilibrium point) *The index of a regular equilibrium point $\bar{x}$ is the sign of the determinant of $-J(\bar{x})$:*

$$\text{ind}(\bar{x}) = \text{sign}\Big(\det\big(-J(\bar{x})\big)\Big)$$

Definition 5 (Degree of a system) *The degree of a dynamical system $\dot{x} = f(x)$, over a set $U \in \mathbb{R}^n$, having equilibria $\bar{x}_i$, $i = 1, ..., m$, is defined as:*

$$\deg(f) = \sum_{i=1}^{m}\{\text{ind}(\bar{x}_i), \bar{x}_i \in U, f(\bar{x}_i) = 0\} ,$$

where $\bar{x}_i$ are regular equilibria.

Theorem 2 *A dissipative dynamical system $\dot{x} = f(x)$ defined on $\mathbb{R}^n$ has degree $+1$ with respect to any bounded open set containing all its equilibria.*

Since systems (S1), (S2), and (S3) are dissipative, by Theorem 2 all have degree $+1$. We further note that the Jacobian matrices of our systems are row equivalent to the identity matrix and thus always invertible for any choice of (positive) parameters and equilibria. Therefore, all equilibria are regular. To determine the index of each equilibrium point, we need not know the value of the equilibrium itself, since in general

$$\text{ind}(\bar{x}) = \text{sign}\Big(\det\big(-J(\bar{x})\big)\Big) = \text{sign}\Big(\det\big(\lambda\boldsymbol{I} - J(\bar{x})\big)\Big), \text{ with } \lambda = 0.$$

Therefore, the index of an equilibrium corresponds to the sign of the constant term in the system's characteristic polynomial $p_J(\lambda) = \det(\lambda I - J(\bar{x}))$. For any choice of the parameters (reaction rates) in systems (S1), (S2), and (S3), the $p_J(\lambda)$ have coefficients that are all positive except the constant term, which may be positive or negative. Thus, the sign of the constant term determines the index of the corresponding equilibrium. Finally, we note that the sign of the constant term in the characteristic polynomial also determines the stability properties of the corresponding equilibrium due to the particular structure of the Jacobians under consideration; we can state the following lemma [6]:

Lemma 1 *Any single equilibrium of systems* (S1)*,* (S2)*, and* (S3) *is unstable if and only if the constant term of the characteristic polynomial $p_J(\lambda)$ is negative. Instability can only be driven by a simple, real (positive) eigenvalue.*

Proof The linearization of systems (S1), (S2), and (S3) define positive linear systems, where the Jacobians J_{md}, J_{dd}, and J_{pf} (given above as (S18), (S19), and (S20)) are similar to Metzler matrices. Therefore, these Jacobians always have a real dominant eigenvalue, i.e. $\lambda_{max} > \mathcal{R}e(\lambda_i)$, $\forall \lambda_i \in J$ [7].

The coefficients of characteristic polynomials $p_{Jmd}(\lambda)$, $p_{Jdd}(\lambda)$, and $p_{Jpf}(\lambda)$ are all real and all positive with the exception of the constant terms, which can be positive or negative. If the constant term of each $p_J(\lambda)$ is negative, then we know that $p_J(0) < 0$ and it is real. In the limit $\lambda \to \infty$, $p_J(\lambda) > 0$ because all other coefficients are positive. Thus, there must be at least one point in the right half plane that is a root of $p_J(\lambda)$. Thus, all our systems unstable, and because the various Js are similar Metzler matrices, their largest roots must be real.

If the system is unstable, then the characteristic polynomial must have at least one root with positive real part. *Ab absurdo*, suppose the constant term is positive. Then instability can only occur with a pair of complex conjugate eigenvalues with positive real part. This is impossible because the Jacobian is a Metzler matrix and the dominant eigenvalue must be real. Thus, the constant term of the characteristic polynomial must be negative. ∎

We can now finish our stability analysis. Our systems all have degree +1 (Theorem 2), thus when three equilibria are present their indices must be equal to +1, +1, and -1 so that their sum is +1 (we recall that all equilibria of our systems are regular). Since the index is equal to the sign of the constant term in the characteristic polynomial, a positive index is associated with a stable equilibrium and a negative index is associated with an unstable equilibrium, and we can conclude that, with three equilibria, our systems are bistable. Note that the unstable point does not admit local oscillatory behaviors, because local instability is driven by a real eigenvalue (Lemma 1). As an alternative argument, we can also simply note that our systems are monotone—for any choice of parameters the Jacobians are similar to Metzler matrices, a property that defines a monotone system with respect to the positive orthant [8, 9]—and a monotone system does not admit oscillatory behaviors.

9 Computational support for Sturm's theorem results

For both toggle circuits, and for each of the valid combinations of $\text{sign}(\mathcal{F}, 0)$ and $\text{sign}(\mathcal{F}, +\infty)$, 1000 random values of $\widehat{X_{1tot}}$ and $\widehat{X_{2tot}}$ were selected from inside and outside of the predicted bistable regions and plugged in to the appropriate equilibrium polynomial (Eq. (3) or (4)) which were then solved numerically. In all cases the number of equilibria found perfectly matched the number determined by Sturm's theorem. It is worth noting that the time required to test $\{\widehat{X_{1tot}}, \widehat{X_{2tot}}\}$ pairs scales linearly with the number of pairs, so while testing a small number can be done relatively quickly, as the number of pairs becomes appreciable the time can be significant—up to 3 hours to test 600,000 random values of $\widehat{X_{1tot}}$ and $\widehat{X_{2tot}}$.

We may also computationally check the stability of the various steady states using the circuits' Jacobian J and characteristic polynomial $p_J(\lambda) = \det(\lambda \boldsymbol{I} - J)$. An equilibrium point is locally stable (unstable) if and only all (some) of the roots of $p_J(\lambda) = 0$ are in the open left-half (closed right-half) of the complex plane. It was also recently shown that if all off-diagonal components of the Jacobian are nonnegative (that is, it is a Metzler matrix), or if the Jacobian may be transformed to have such a form, then any equilibrium is unstable if and only if the constant term of $p_J(\lambda)$ has a sign opposite to that of all other terms in $p_J(\lambda)$ [6]. We use this $p_J(\lambda)$ constant term condition to confirm that each bistable solution set contains one solution representing an unstable steady state.

The inequalities that satisfy the $p_J(\lambda)$ constant term condition are:

$$
\begin{aligned}
\widehat{P_{1eq}}^4 &+ 4\widehat{P_{1eq}}^3 + 2\widehat{P_{1eq}}^2(\widehat{X_{2tot}}^2 + 3) \\
&+ \widehat{P_{1eq}}\left(4 - 2(\widehat{X_{1tot}} - 2)\widehat{X_{2tot}}^2\right) - 2(\widehat{X_{1tot}} - 1)\widehat{X_{2tot}}^2 + \widehat{X_{2tot}}^4 + 1 < 0
\end{aligned}
\tag{S21}
$$

and

$$
\left(\widehat{P_{1eq}}^4 + 2\widehat{P_{1eq}}^2 + \widehat{X_{2tot}}^2 + 1\right)^2 - 4\widehat{P_{1eq}}(\widehat{P_{1eq}}^2 + 1)\widehat{X_{1tot}}\widehat{X_{2tot}}^2 < 0
\tag{S22}
$$

for the MD and DD toggles, respectively. For each bistable solution set found we substituted the values $\widehat{X_{1tot}}$, $\widehat{X_{2tot}}$, and $\widehat{P_{1eq}}$ into Eqs. (S21) and (S22) and confirmed that only one of the three solutions satisfies the appropriate instability condition, supporting our claim that for the systems under consideration, if three roots to the equilibrium polynomial can be found, then two must be stable and one must be unstable.

References

[1] Siegal-Gaskins D, Mejia-Guerra MK, Smith GD, Grotewold E. Emergence of switch-like behavior in a large family of simple biochemical networks. PLoS Comput Biol. 2011 May;7(5):e1002039.

[2] Farina L, Rinaldi S. Positive linear systems: theory and applications. vol. 50. John Wiley & Sons; 2011.

[3] Hale JK. Theory of functional differential equations. No. v. 3 in Applied Mathematical Sciences Series. Springer Verlag GmbH; 1977.

[4] Hofbauer J. An index theorem for dissipative semiflows. Journal of Mathematics. 1990;20(4).

[5] Khalil HK. Nonlinear Systems. Pearson Higher Education; 2002.

[6] Mardanlou V, Tran CH, Franco E. Design of a molecular bistable system with RNA-mediated regulation. Decision and Control (CDC), 2014 IEEE 53nd Annual Conference on. Accepted;.

[7] Son NK, Hinrichsen D. Robust stability of positive continuous time systems. Numerical functional analysis and optimization. 1996;17(5-6):649–659.

[8] Smith HL. Monotone Dynamical Systems: An Introduction to the Theory of Competitive and Cooperative Systems. American Mathematical Society; 2008.

[9] Sontag E. Monotone and near-monotone biochemical networks. Syst Synth Biol. 2007 Apr;1(2):59–87.